Mirouze, Isabell; Ricci, Sophie; Goutal, Nicole

The impact of observation spatial and temporal densification in an ensemble Kalman Filter

The impact of observation spatial and temporal densification in an ensemble Kalman Filter

Isabelle Mirouze, Sophie Ricci

CERFACS / CNRS UMR 5318
Toulouse, France
isabelle.mirouze@cerfacs.fr

Nicole Goutal

LNHE-EDF, -LHSV
Chatou, France

***Abstract*—To reduce uncertainties in a modelled system, data assimilation strongly relies on the availability of observations, and its performance depends directly on the spatial density, the frequency, and the quality of these observations. Yet, rivers are rather poorly observed. The SWOT (Surface Water and Ocean Topography) mission, to be launched in 2021, is expected to provide global water level observations at a high-resolution coverage for rivers down to 50-meter wide.**

In order to highlight the merits of these future observations, we compare the performance of an Ensemble Kalman Filter on a 50-kilometre reach of the Garonne (South of France) when only hourly water height gauge measurements are available in the middle of the reach, and when complementary SWOT-like observations are available. A 10-kilometre spatial average with frequencies of 3 and 1 days are tested in the framework of twin experiments. Results show that assimilating the SWOT-like observations allows the ensemble size to be reduced without losing accuracy. With a better correction of the friction coefficients and the upstream discharge, the water height systematic bias is cancelled out and the root mean square error is decreased, *i.e.* the deviation to the reference is reduced. The beneficial impact of the SWOT-like observations holds in the 12 first hours of the forecast.

I. Introduction

Data assimilation aims to reduce the uncertainties in a modelled system by correcting the initial conditions, the boundary conditions and the parameters of this system. Among the different schemes available, the Ensemble Kalman Filter (EnKF; [1]) has the advantage of not requiring any adjoint model. Moreover, the background error covariance matrix being calculated using the ensemble, the analysis benefits from its flow-dependency. Like any Monte Carlo-based methods however, it requires a large number of members to estimate the background error covariance matrix accurately enough, which increases its cost.

Data assimilation also strongly relies on the availability of observations, and its performance depends directly on the spatial density, the frequency, and the quality of these observations. Yet, rivers are rather poorly observed. Observations come mainly from limnimetric *in situ* stations, which provide water height measurements and, for few of them, discharge measurements. However, the network coverage is not global, and not necessarily sustained, as shown in Fig. 1. In some regions, data can be difficult to access due to political instabilities, or financial fees. Even in countries such as USA, Canada, France or UK who are maintaining a sustainable network, entire sections of rivers are not watched on.

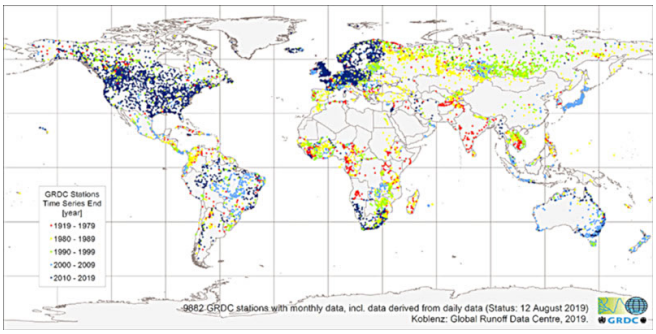

Fig. 1: Global Runoff Data Centre[2] stations with monthly data, status on 12 August 2019. Time series end between 1919 and 1979 (red), 1980 and 1989 (yellow), 1990 and 1999 (green), 2000 and 2009 (light blue), 2010 and 2019 (dark blue).

Nadir altimeters on board satellites such as Jason-2 can also provide water level measurements, but they have an incomplete and low-resolution spatial coverage that make them adapted for major rivers only. The SWOT (Surface Water and Ocean Topography) mission[1] of CNES (Centre National d'Etudes Spatiales) and NASA (National Aeronautics and Space Administration), to be launched in 2021, is expected to provide water level measurements with a global and high-resolution spatial coverage, decreasing thus the width of potentially observed rivers down to 50 meters. The temporal revisit will be of 21 days, with a 4-day insight on catchments at our latitudes. The accuracy of the water level measurements, will depend on the product delivered. For example, for 10-kilometre reach average observations, the accuracy is expected to be 10 cm.

1: https://swot.cnes.fr/en/mission-1, https://swot.jpl.nasa.gov/mission.htm

2: https://www.bafg.de/GRDC/EN/Home/homepage_node.html

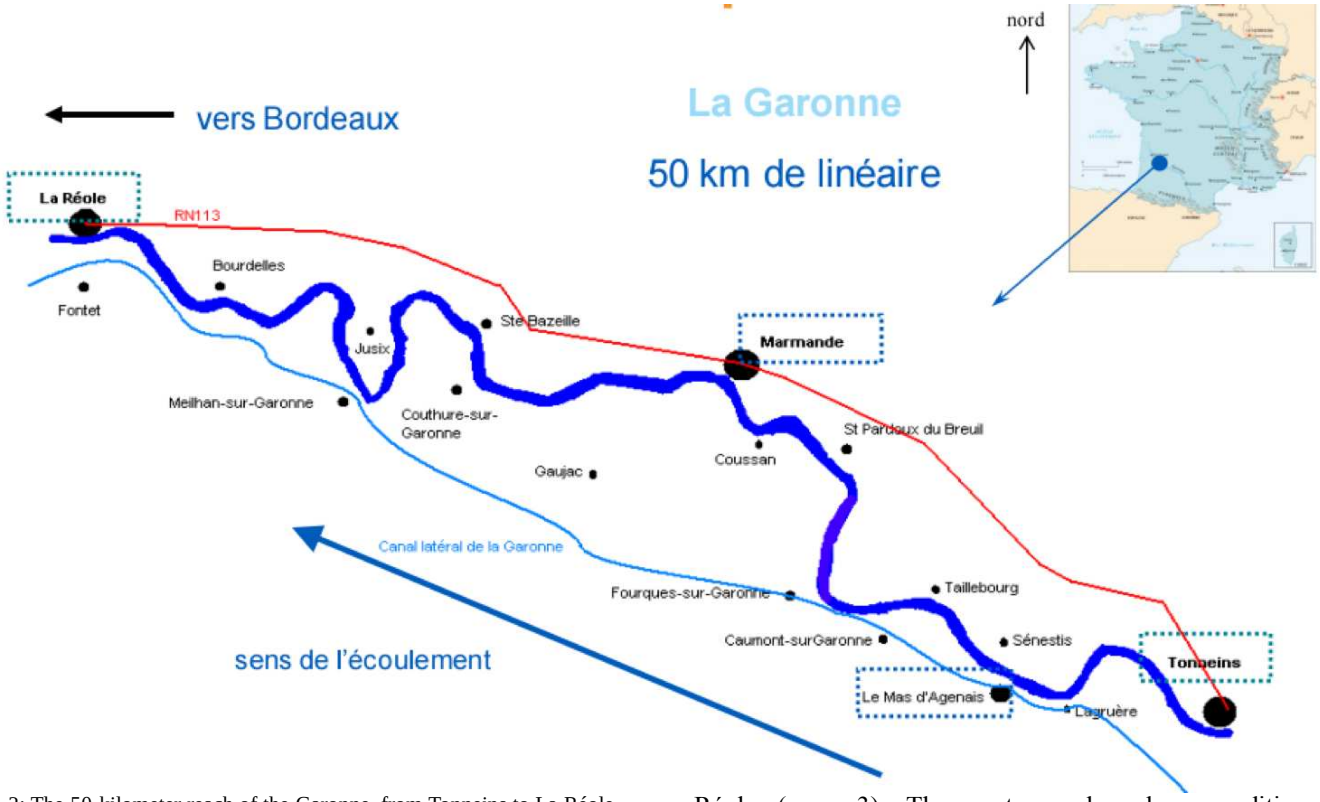

Fig. 2: The 50-kilometer reach of the Garonne, from Tonneins to La Réole. Credit: A. Besnard and N. Goutal, simHydro, 2010.

In this paper, we study the impact on the reanalyses and forecasts of densifying the observation network in space and time, using SWOT-like observations in twin experiments. To do so, we use the Smurf (System for Modelling with Uncertainty Reduction, and Forecasting; [2]) framework, an open source modular system developed in Python at Cerfacs for running and cycling data assimilation systems. The focus of the study is a 50-kilometer reach of the Garonne, from Tonneins to La Réole, modelled with the 1D hydrodynamics solver Mascaret [3].

The paper is organised as follows: section 2 provides information on the framework and the configuration used, whilst section 3 describes the experiments and their results; finally, section 4 summarises the study and gives some conclusions.

II. Framework and configuration

A. The numerical model Mascaret

Mascaret is a Fortran code that solves the Saint-Venant equations with a finite difference scheme, in order to simulate one-dimensional free surface hydraulic systems. For our configuration, the equations are solved with a time step of 30 minutes and a spatial resolution of about 100 m (463 nodes).

The study focusses on a 50-kilometer reach of the Garonne, from Tonneins to La Réole as shown in Fig. 2. The Strickler coefficient $\boldsymbol{Ks}$ is uniformly defined over three areas, from Tonneins to Mas d'Agenais (zone 1), from Mas d'Agenais to Marmande (zone 2), and from Marmande to La Réole (zone 3). The upstream boundary condition is prescribed with a discharge time series $\boldsymbol{Q_{up}(t)}$ at Tonneins created on purpose to represent a sequence of high and low flows (Fig. 3). The downstream boundary condition is a rating curve at La Réole.

B. The Ensemble Kalman Filter

The stochastic version of the EnKF is used to correct the three Strickler coefficients and the time-varying upstream discharge. The idea is to construct an ensemble of corrected simulations of size $\boldsymbol{N}$ whose mean represents the best estimate of the hydraulic state of the river. The ensemble is constructed by generating perturbations with Batman-OT (Bayesian Analysis Tool for Modelling and uncertAinty quaNtification – Open Turns; [4]). For the Strickler coefficients ($\boldsymbol{Ks_1}$, $\boldsymbol{Ks_2}$, $\boldsymbol{Ks_3}$), scalar perturbations are drawn from a uniform law centred on the analysis mean with a range of ± 5 $m^{1/3}s^{-1}$. The upstream discharge time series $\boldsymbol{Q_{up}(t)}$ is perturbed by a Gaussian process applied to a reference time series. A principal component analysis is performed on a sample of 10000 processes with chosen features. In this study we chose a Matérn function with a smoothness parameter $\eta = 0.5$ (exponential) and length scale of 1 day. A truncation is then applied according to a chosen threshold to keep a determined number of modes (3 in this study). To generate a sample of perturbations for $\boldsymbol{Qup(t)}$, the truncated principal components transformation is sampled from a centred normal distribution with a chosen standard deviation, before being applied to the weights. To minimise the cost of the analysis calculation, we chose to control the components of the transformation ($\boldsymbol{c_1}$, $\boldsymbol{c_2}$, $\boldsymbol{c_3}$) rather than the time series itself, which leads to a control vector

$$\boldsymbol{x = (Ks_1, Ks_2, Ks_3, c_1, c_2, c_3)^T}. \quad (1)$$

A 50-day simulation is carried out over the sliding windows of 3 hours (assimilation cycle) every hour, with a 24-hour forecast launch at the end of each window as shown on Fig. 4. For example, a first assimilation cycle is conducted from T_0 to T_3 with a forecast from T_3 to T_{27}, then a second cycle is performed from T_1 to T_4 with a forecast from T_4 to T_{28}, and so on. The sliding windows imply that the same observations are used within different assimilation cycles. For each cycle, the assessment of the system is performed with respect to the end of the windows. For example, the date T_4 with lead time 0h and 1h is picked into the second assimilation cycle and first forecast, respectively. At the start of the simulation, all members of the ensemble have the same hydraulic state. The members will diverge however due to the differences between their control vectors (1). Note that the perturbations are generated at the start of each assimilation cycle to avoid the ensemble to collapse (no inflation used). For the upstream discharge a common time series is kept to which perturbations are added for each member.

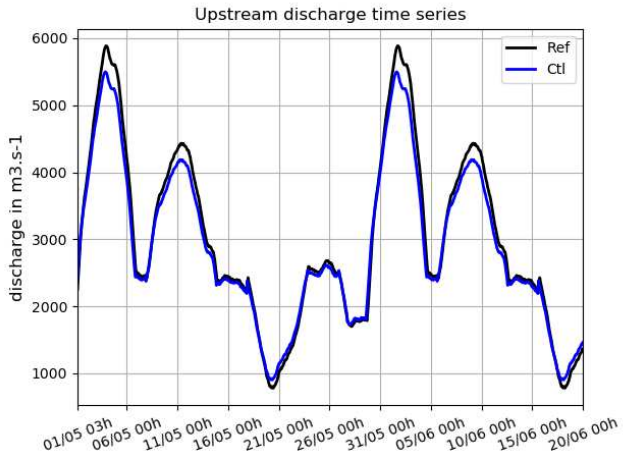

Fig. 3: Reference (black line) and perturbed (blue line) upstream discharge at Tonneins.

During the assimilation cycle an analysis $\boldsymbol{x^a}$ for each member $\boldsymbol{i = 1, \ldots N}$ is firstly calculated

$$\boldsymbol{x^a_i = x^b_i + K\,(y^o_i - y^b_i)}, \qquad (2)$$

where $\boldsymbol{x^b}$ is the background control vector and $\boldsymbol{y^b = Hx^b}$ its counterpart in the observation space. $\boldsymbol{H}$ is the observation operator that maps the control vector space onto the observation space. In our case, $\boldsymbol{H}$ is constituted of the model Mascaret providing the water height at the time and possibly interpolated location of the observation. The observation vector $\boldsymbol{y^o}$ gathers all observations available within the window. This vector is then perturbed for each member according to a normal distribution with zero mean and the prescribed observation error covariance matrix $\boldsymbol{R}$. We have considered here a diagonal matrix (no correlation between observation errors). In (2) the correction (increment) to the background control vector is defined by the misfit between the observations and the background control vector counterpart (innovation) weighted by the Kalman gain

$$\boldsymbol{K = BH^T\,(HBH^T + R)^{-1}},$$

where

$$\boldsymbol{BH^T = E[(x^b - E[x^b])(y^b - E[y^b])^T]}, \qquad (3)$$

$$\boldsymbol{HBH^T = E[(y^b - E[y^b])(y^b - E[y^b])^T]}, \qquad (4)$$

are estimated from the ensemble. $\boldsymbol{E[.]}$ is the expectation operator.

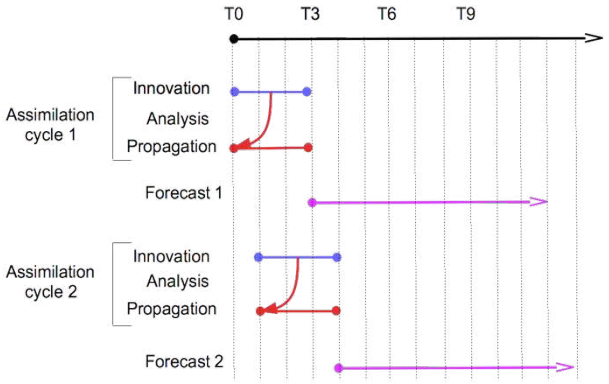

Fig. 4: Cycling of the simulation with 3-hourly sliding windows.

The corrected Strickler coefficients are taken into account and the uniform law used to generate the associated perturbations is re-centred about their analysis mean. The analysed principal components of each member are used to generate an analysed perturbation for the upstream discharge time series $\boldsymbol{Q_{up}(t)}$ that is taken into account. The common time series is corrected by the mean of these perturbations. The ensemble members are then propagated again from the start of the same window, before a 24-hour forecast is launched. During the forecast, the last upstream discharge of the assimilation cycle is persisted, assuming no upstream discharge forecast is available.

C. The observations

The observations used in this study are synthetic, generated from the reference run of the twin experiments (see section III) with a perturbation drawn from a centred normal distribution with standard deviation of 10 cm. A first set of hourly water height at node 221 is defined to represent the ***in situ*** station of Marmande. The SWOT-like observations are simulated as if they were coming from limnimetric stations at nodes 47, 142, 236, 334, 423, representing a distance between stations of about 10 km. Two sets of data have been generated: one with daily observations, and one with observations every 3 days. The error standard deviation of 10 cm corresponds to the requirement of the SWOT mission for a 10-kilometre reach average. Preliminary tests with shorter spatial average (and appropriate error standard deviation, ***e.g.*** 20 cm for a 5-kilometre reach average) were conducted and showed that improvements in the root mean square (rms) error with respect

to the reference run were more linked to the frequency of the observations rather than the spatial average. Therefore, we chose to limit this study to a 10-kilometre reach average.

D. The Smurf framework

The experiments of this study have been carried out using Smurf[3], an open source code developed in Python. It is used to run and cycle data assimilation systems in a modular way. Smurf is organised around three super classes for the numerical models, the data assimilation schemes and the observation instruments. Any new item can be easily plugged in by defining a child class that will override as many methods as necessary.

A specific python class has been developed for Mascaret in order for Smurf to set parameters, to launch the simulation and to retrieve variable values at specific times, through Application Programming Interfaces (API). A class ***Gauge*** has also been implemented to handle the observations coming from limnimetric stations. It manages the observation files and some basic checking such as the observation time with respect to the assimilation cycle currently processed. The EnKF used in this study is part of Smurf and available for any systems.

The possibility of integrating the ensemble members simultaneously in parallel (innovation calculation, analysis propagation, and forecast) has been used in this study, reducing significantly the elapsed time for the assimilation experiments.

III. RESULTS OF TWIN EXPERIMENTS

Twin experiments have been conducted to assess the impact of densifying the observation network over time, in the prospect of the SWOT mission.

A. Experiments

The Reference experiment (Ref) is a deterministic simulation without data assimilation. The Strickler coefficients are set to $Ks_1 = 40$, $Ks_2 = 32$ and $Ks_3 = 33$, and the upstream discharge time series $Q_{up}(t)$ is the originally designed one (Fig. 3, black line). This experiment is considered as the "truth" and is used to generate observations with a noise corresponding to the error standard deviation defined (10 cm).

The Control experiment (Ctl) is also a deterministic simulation without data assimilation. However, it respects the cycling of 3-hourly sliding windows in order to launch 24-hour forecasts (with persisted upstream discharge) at the end of each window. Although the initial hydraulic state is the same as Ref, the Strickler coefficients are set to $Ks_1 = 30$, $Ks_2 = 40$ and $Ks_3 = 40$, and the original upstream discharge time series $Q_{up}(t)$ is perturbed to simulate some inaccuracies (Fig. 3, blue line). This experiment is considered as the one to improve towards Ref.

Different experiments with data assimilation have been carried out. They are all run with the same configuration as Ctl for the Strickler coefficients and the upstream discharge, but will diverge from it due to the corrections brought sequentially by the assimilation. A first experiment (Ais) assimilates only the hourly in situ data at Marmande. The second and third experiments (A3d and A1d) assimilate SWOT-like observations every 3 and 1 days, respectively. The two last experiments (Ais3d and Ais1d) assimilate both the hourly in situ data at Marmande and the SWOT-like observations every 3 and 1 days, respectively.

Each simulation is run during 52 days. The first two days are considered as a spinup to allow for the hydraulic state to stabilise with respect to the initial conditions and parameters. As a consequence, Ref and Ctl (and hence the assimilation runs) will diverge slightly. Therefore, the period of assessment goes for 50 days, from the hypothetical dates of 1st May to 20th June.

B. Size of the ensemble

The choice of the ensemble size for an EnKF algorithm is crucial. Too small, it will lead to inaccurate covariance estimates and hence a poor performance, although technics such as localisation are available to address this issue (***e.g.*** [5]). Too big, it will lead to unaffordable costs. The experiment Ais assimilating only ***in situ*** observations at Marmande is representative of what can currently be done. Therefore, it was run with 50 (Ais) and 100 (Ais100) members, in order to assess the impact of the covariance estimate accuracy.

As expected, both experiments are well constraining the water height at Marmande. Whereas the water height stays close to Ctl for both runs at La Réole, a large difference can be seen upstream at Mas d'Agenais. With 50 members only (Fig. 5), the water height drifts slowly from Ctl, reaching a difference with Ref greater than 3 meters at the end of the period. With 100 members (Fig. 6), there is no obvious drift. This drift is due to incorrect analyses for the Strickler coefficients ***Ks1*** and ***Ks2*** as shown in Fig. 10 and Fig. 11 (brown line), respectively. This issue is a consequence of spurious correlations in the estimate of the covariances (3) and (4). Because Ais100 uses twice the number of members, the estimates are more accurate and these spurious correlations, though still existing, are smaller and hence, less detrimental. Nevertheless, evidence of a drift for Ais100 might have been spotted on a longer simulation period. Note that the upstream discharge time series is less sensitive to the problem, thanks to the fact that the correction is not done directly, but on hyperparameters. Fig. 9 shows the evolution of the global rms of the water height error with respect to Ref for Ctl and the ensemble means of Ais and Ais100. After a month, the rms for Ais is higher than for Ctl, whilst Ais100 stays below. The degradation in the rms for Ais is mainly due to a bias increase. Spatially, this bad performance of Ais is restricted to the first and second zones (Fig. 7), ***i.e.*** upstream of the observation location.

The choice is made to run the other assimilation experiments with 50 members only, since we expect the densification of the observation network to better constrain the problem.

C. Performance of the data assimilation

The performance of the data assimilation is assessed by comparing the mean and the rms of the water height difference

3: https://gitlab.com/cerfacs/Smurf

between the ensemble mean of each experiment with the reference (Ref). These diagnostics are performed by summing over time (Fig. 7 and Fig. 8), over location (Fig. 9), or both (Fig. 13, Fig. 14 and table hereafter). The global performance is summarised in the following table, with a focus at Marmande. As expected, the error is significantly reduced when data assimilation is used (except for Ais), although the performance is not spatially homogeneous (Fig. 7).

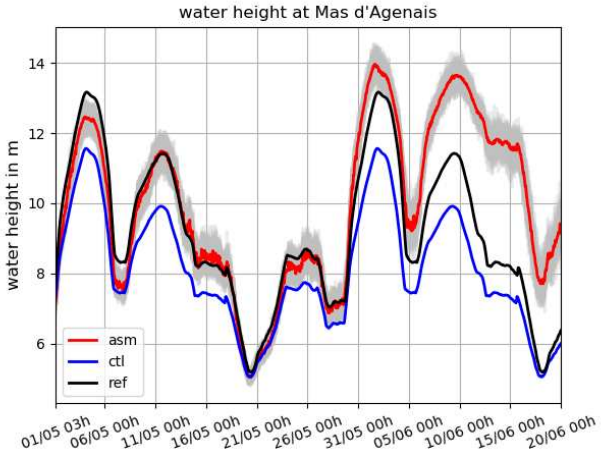

Fig. 5: Water height at Mas d'Agenais for Ref (black line), Ctl (blue line), and Ais (grey lines for the members, red line for the ensemble mean).

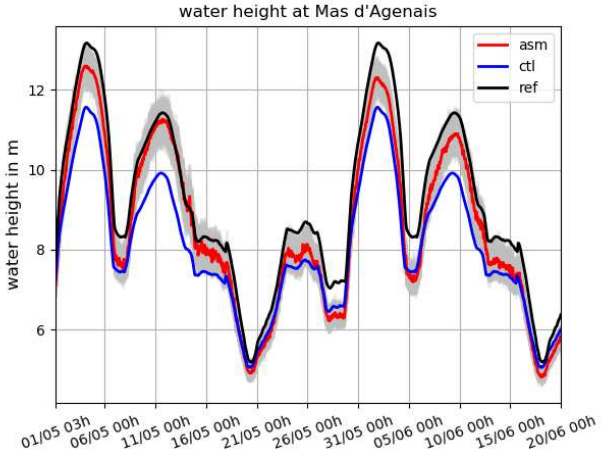

Fig. 6: Water height at Mas d'Agenais for Ref (black line), Ctl (blue line), and Ais100 (grey lines for the members, red line for the ensemble mean).

D. Performance of the data assimilation

The performance of the data assimilation is assessed by comparing the mean and the rms of the water height difference between the ensemble mean of each experiment with the reference Ref. These diagnostics are performed by summing over time (Fig. 7 and Fig. 8), over location (Fig. 9), or both (Fig. 13, Fig. 14 and table 1). The global performance is summarised in the following table, with a focus at Marmande. As expected, the error is significantly reduced when data assimilation is used (except for Ais), although the performance is not spatially homogeneous (Fig. 7).

TABLE 1: MEAN AND RMS ERROR WITH RESPECT TO REF FOR WATER HEIGHT

Experiment	Global (mm)		Marmande (mm)	
	Mean	Rms	Mean	Rms
Ctl	-696	854	-844	904
Ais100	-161	312	0	69
Ais	337	907	9	70
A3d	-104	363	-119	373
Ais3d	8	418	5	73
A1d	-29	199	-16	200
Ais1d	-16	157	2	69

In the first zone the rms error for Ctl is small close to Tonneins (45 cm) but increases rapidly (up to more than 1 m) due to the erroneous Strickler coefficient. In zones 2 and 3 the rms stays high although decreasing slowly. Near La Réole, the rms decreases again (35 cm) constraint by the rating curve. The large rms is mainly due to a systematic bias (Fig. 8). Between Tonneins and Marmande, the assimilation manages to reduce the rms for all experiments, except for Ais as mentioned in the previous section. We note nevertheless a slight increase in the rms for Ais3d, but this is mainly coming from the 10 first days of the period, the assimilation struggling a bit to adjust to occasional observations as shown in Fig. 9.

At Marmande, the significant bias of Ctl is almost cancelled out by the assimilation, reducing significantly the rms. This is especially true for the experiments assimilating hourly data at Marmande. For the latter, the constant Strickler coefficient of the third zone and the water height spatial correlations allow for the correction to hold downstream until a few kilometres before La Réole, where the rating curve takes precedence.

Assimilating only SWOT-like data (A3d and A1d) shows a good behaviour at all locations, with a rms about 40 cm and 20 cm depending on the observation frequency (3 days or 1 day, respectively). However, downstream of Marmande these experiments are not as successful as the experiments assimilating hourly observations at Marmande which show a rms smaller than 10 cm. It is interesting to note that all the experiments assimilating SWOT-like observations perform better than Ais100 upstream of Marmande, although their ensemble is twice smaller. The mean error in particular, is almost cancelled out. Fig. 9 shows that the assimilation struggles especially when there are rapid changes in the flow, as shown by the upstream discharge time series on Fig. 3.

The control vector (1) describes the variables that are corrected by the assimilation. The principal components of the transformation (***c1***, ***c2***, ***c3***) do not have a "truth" value since they generate a perturbation, and cannot hence be compared to a reference, unlike the upstream discharge time series ***Qup(t)*** itself. The time series for each assimilation experiments are not sufficiently well corrected for their analysis mean to reach the reference values (not shown). In particular, the high flows are still underestimated by a few hundreds of m3s-1. The analysis mean of the Strickler coefficients ***Ks_1, Ks_2 and Ks_3*** can be compared directly to the "truth" values of the Ref experiment. Fig. 10, Fig. 11 and Fig. 12 show the evolution of their analysis mean. The patterns for A3d and A1d are similar to Ais3d and Ais1d, respectively, and are therefore not shown.

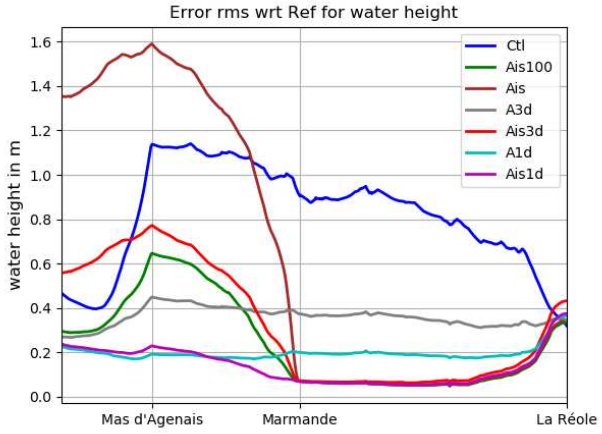

Fig. 7: Global rms of the water height error with respect to Ref depending on the location for Ctl and the ensemble mean of all experiments.

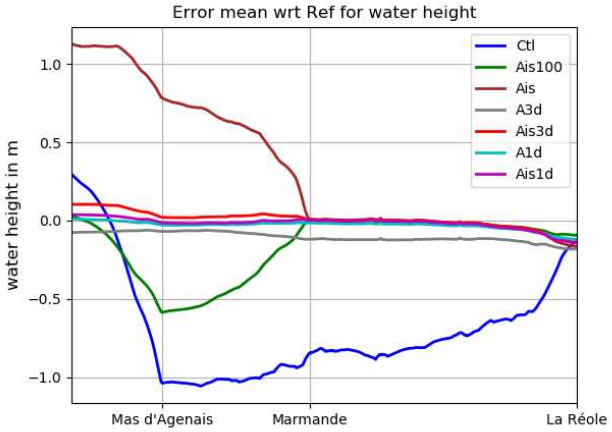

Fig. 8: Global mean of the water height error with respect to Ref depending on the location for Ctl and the ensemble mean of all experiments.

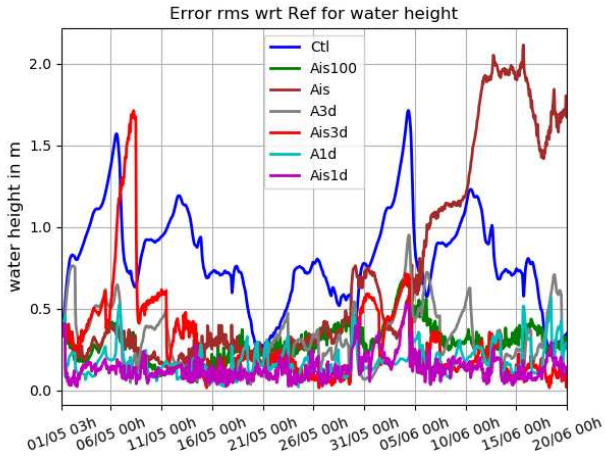

Fig. 9: Evolution of the global water height rms error with respect to Ref for Ctl and the ensemble mean of the assimilation experiments.

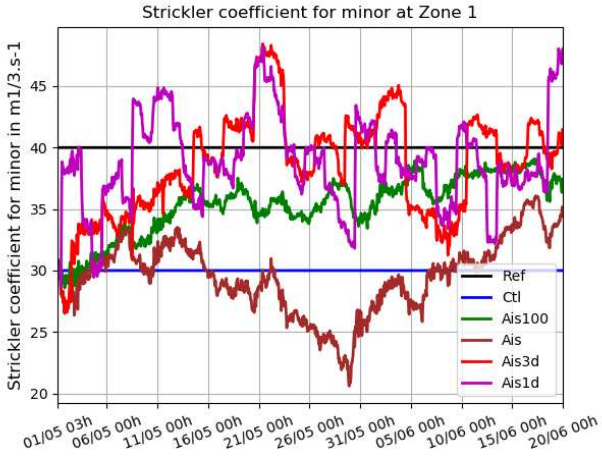

Fig. 10: Evolution of the analysis mean for Ks_1 in Ais100 (green line), Ais (brown line), Ais3d (red line) and Ais1d (pink line). The "truth" and erroneous values are shown by the black and blue lines, respectively.

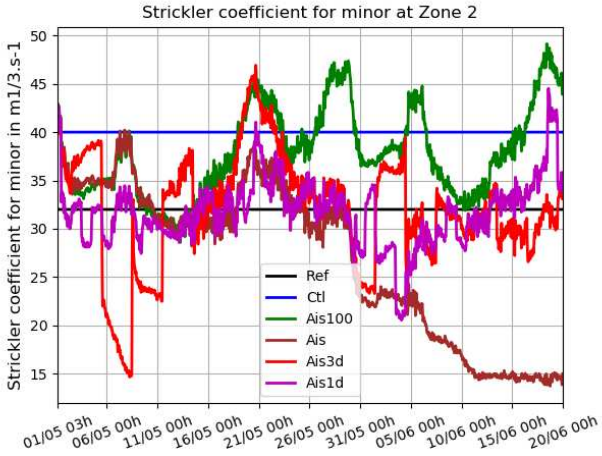

Fig. 11: Evolution of the analysis mean for Ks_2 in Ais100 (green line)), Ais (brown line), Ais3d (red line) and Ais1d (pink line). The "truth" and erroneous values are shown by the black and blue lines, respectively.

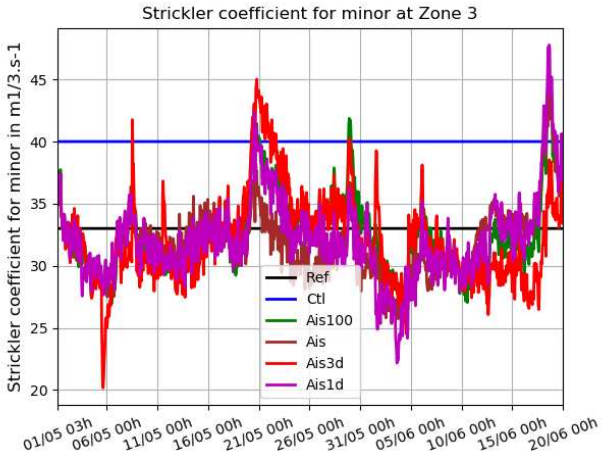

Fig. 12: Evolution of the analysis mean for Ks_3 in Ais100 (green line)), Ais (brown line), Ais3d (red line) and Ais1d (pink line). The "truth" and erroneous values are shown by the black and blue lines, respectively.

Whilst the assimilation manages to correct Ks_3 towards its reference value for all experiments, it clearly struggles to do so for Ks_1 and Ks_2 when only hourly ***in situ*** data at Marmande are available. The SWOT-like observations have a clear positive impact on the analysis. The more frequent the observations, the better the impact is, accelerating the convergence for Ks_1 and reducing the amplitude of the oscillations for Ks_2. It is worth mentioning that even if the upstream discharge time series and the Strickler coefficients are not exactly to their "truth" value, the water height at the location of frequent observations (Marmande in particular) is still close to the values of Ref. This is due to the well-known issue of equifinality [6].

E. Forecasts

At the end of each 3-hourly assimilation window, a 24-hour forecast is launched for each member of the ensemble, with the Strickler coefficients corrected during the assimilation cycle. The upstream discharge value at the end of the assimilation cycle is persisted during the forecast.

Fig. 13 and Fig. 14 show the global water height rms and mean error, respectively, with respect to Ref, for Ctl and all the assimilation experiments at hourly lead times (ensemble mean). For Ctl, the rms is about 85 cm during 12 hours, and starts then increasing reaching 1.1 m at the end of the forecast. If most of the error comes from a bias in the first half of the forecast, this bias increases only slightly in the second half. For the reasons exposed in section III-B, assimilating only ***in situ*** data at Marmande with 50 members, gives a higher rms than Ctl. During the first 12 hours, the other experiments benefit from the performance of their own assimilation cycle and hence have a smaller rms (and mean) than Ctl. Their respective performance are similar in the second half of the forecast, with a rms increasing faster than Ctl. After 24 hours, their rms is still about 20 cm smaller than Ctl. Extrapolating the data, we can estimate that the assimilation would lose its impact on the forecast after a lead time of about 30 to 32 hours. Note that the mean for all experiments is quite stable.

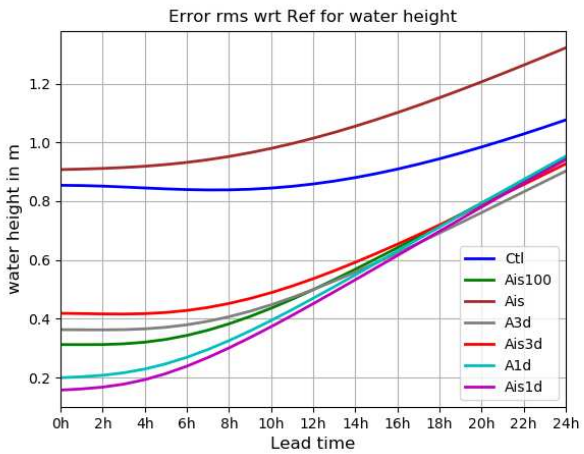

Fig. 13: Global water height rms error with respect to Ref for the ensemble mean of the assimilation experiments.

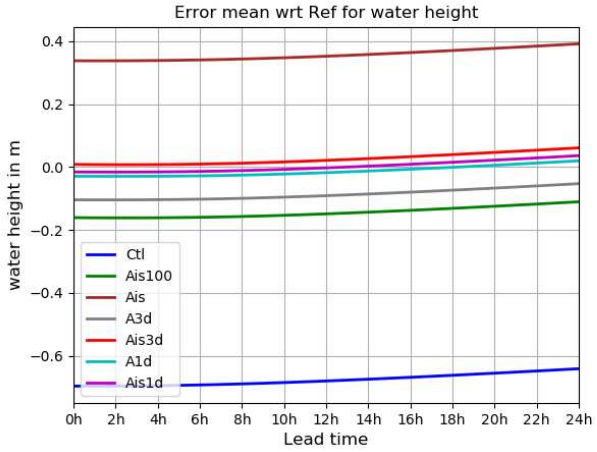

Fig. 14: Global water height mean error with respect to Ref for the ensemble mean of the assimilation experiments.

IV. CONCLUSION

We have studied the potential impact of the observation spatial and temporal densification on a data assimilation system using an EnKF, in terms of accuracy of reanalysis and forecast. On a 50-kilometre reach of the Garonne, we compared the assimilation of hourly ***in situ*** observation water height at Marmande to the assimilation of SWOT-like water height observations every 10 kilometres with a frequency of 3 and 1 days in the framework of twin experiments.

Having observations distributed regularly along the reach allows a smaller ensemble to have the same performance in terms of rms as a specified one. The decrease in ensemble size depends on the frequency of these regular observations. It is unlikely that SWOT observations will be available at a higher frequency than daily. Therefore, hourly data from limnimetric stations will still be useful to reduce the rms error at their locations and downstream of them.

Assimilating SWOT-like observations constrains better the system and the Strickler coefficients are hence rather well corrected, whereas assimilating ***in situ*** data only manages to correct the Strickler coefficient of the third zone. We did not see any improvement on the upstream discharge time series however, probably because of the equifinality issue and the correction method. Nevertheless, this better set of parameters cancels out the systematic bias existing upstream of the limnimetric station. The positive impact of the SWOT-like observations holds during the first 12 hours of the forecast.

The SWOT mission scheduled for a launch in late 2021 will allow us to have observations of water level regularly distributed in space for rivers down to 50-metre wide. This will be an opportunity to improve the reanalyses and forecasts of our hydraulic systems.

ACKNOWLEDGEMENT

This study has been carried out within the Discharge proposal of the SWOT – TOSCA (Terre solide, Océan, Surfaces Continentales et Atmosphère) program of CNES.

The authors are grateful to Matthias De Lozzo who coded the API used by Smurf to manage Mascaret.

REFERENCES

[1] G. Evensen, “Sequential data assimilation with a nonlinear quasi-geostrophic model using Monte Carlo methods to forecast error statistics”, J. Geophys. Res., 1994, vol. 94, pp. 10143–10162.

[2] I. Mirouze and S. Ricci, “Smurf: System for Modelling with Uncertainty Reduction, and Forecasting”, unpublished.

[3] N. Goutal and F. Maurel, “A finite volume solver for 1D shallow water equations applied to an actual river”, Int. J. Numer. Math. Fluids, 2002, vol. 38, pp. 1–19.

[4] P. T. Roy, S. Ricci, R. Dupuis, R. Campet, J.C. Jouhaud, C. Fournier, “BATMAN : Statistical analysis for expensive computer codes made easy”, Journal of Open Source Software, 2018, vol. 3(21), 493.

[5] P. R. Oke, P. Sakov, S. P. Corney, “Impacts of localisation in the EnKF and EnOI: experiments with a small model”, Ocean Dyn., 2007, vo. 57, pp. 32–45

[6] G. Aronica, B. Hankin, K. Beven, “Uncertainty and equifinality in calibrating distributed roughness coefficients in flood propagation model with limited data”, Adv. Water Resour., 1998, vol. 22, pp. 349–365.